Electronic Supplementary Material (ESI) for Physical Chemistry Chemical Physics.

Supplementary Information for

Endo- and Exocytic Budding Transformation of Slow-Diffusing Membrane Domains Induced by Alzheimer's Amyloid Beta.

Masamune Morita, Tsutomu Hamada*, Mun'delanji C. Vestergaard, Masahiro Takagi

Experimental Section

Materials.

Dioleoyl phosphatidylcholine (DOPC), dipalmitoyl phosphatidylcholine (DPPC), cholesterol (Chol), and NBD-DPPE (λex=460 nm, λem = 535 nm) were obtained from Avanti Polar Lipids. N-(rhodamine red-X)-dihexadecanoyl-sn-glycero-phosphoethanolamine triethyl ammonium salt (rho-PE, λex=560 nm, λem=580 nm) and was obtained from Invitrogen. Monomer of Amyloid β protein (Human, 1-42) trifluoroacetate salt (Aβ-42) was purchased from Peptide Institute, and monomer of fluorescent (HiLyte Fluor 488)-labeled Aβ-42 (λex=503 nm, λem = 528 nm) was obtained from Anaspec. Deionized water was obtained using a Millipore Milli Q purification system.

Preparation of Aβ aggregation species.

Monomers of Aβ-42 and fluorescent (HiLyte Fluor 488)-labeled Aβ-42 were dissolved in 0.02 % ammonia solution at 200 μM and stored at -80 ºC. Only in the Aβ localization experiment, fluorescence-labeled Aβ and Aβ were mixed in a molar ratio of 1:1. Monomers of Aβ-42 peptides (final concentration is 80 μM) were diluted in 20 mM Tris/HCl buffer (pH 7.4) and allowed to spontaneously aggregate at 37 ºC for 12 h (to obtain oligomers of Aβ-42). Unless otherwise stated, all analyses were carried out at 25 ºC.

Characterization of Aβ aggregation species.

Aβ assemblies were directly imaged using an atomic force microscopy (AFM) unit (SPA400-SPI3800, Seiko Instruments Inc., Japan) equipped with a calibrated 20 μm xy-scan and 10 μm z-scan range PZT-scanner and a silicon nitride tip (SI-DF3, spring constant=1.6 N/m, frequency resonance=28 kHz, Seiko Instruments Inc.). Prior to analysis, the sample was prepared by dilution with Milli Q to a final concentration of 10 μM. The peptide was then immediately immobilized on a clean mica disk (Furuuchi Chemical Co., Japan), and imaged. All AFM images were obtained in air in dynamic force mode (DFM) at optimal force. All AFM procedures were performed in an automated

moisture-control box with 30–40% humidity.

Preparation of membranes.

Phospholipids dissolved in chloroform/methanol (2:1, v/v) were poured into a glass test tube. The organic solvent was then evaporated under a nitrogen flow and dried under vacuum to make a dry film at the bottom of the test tube. The tube was placed in a desiccator for 3 h to remove the organic solvent. The film was then swollen with 1.25 mM Tris for 24 h at 37 ºC. The final lipid concentration was 0.2 mM.

Microscopic observation

Aβ-peptides were added to lipid vesicles to a final concentration of 5 μM, and visualized using a laser confocal microscope (Olympus FV-1000, Japan) at 25 ºC. Diode lasers (559 and 473 nm) were used to excite rho-PE and NBD-DPPE or fluorescent-labeled Aβ-42, respectively.

1. **Characterization of each Aβ-42 aggregation species**

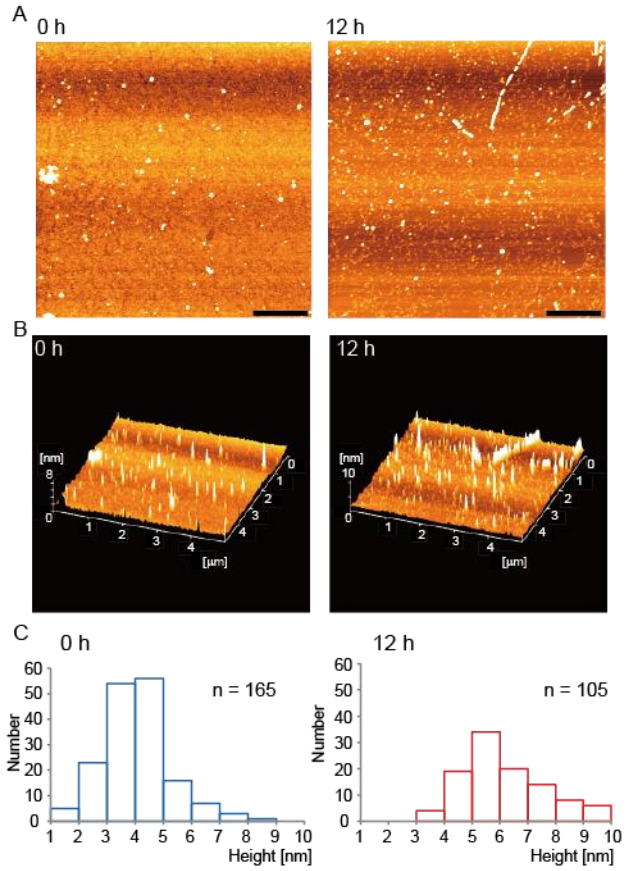

Figure S1 (A,B) Atomic force microscopy (AFM) images of Aβ-42 aggregation species after incubation at 37 ºC in 20 mM Tris (pH 7.4). Monomers (0 h), Oligomers (12 h). (C) Histogram of height for each Aβ aggregation species.

2. Membrane transformation induced by glucose osmotic pressure

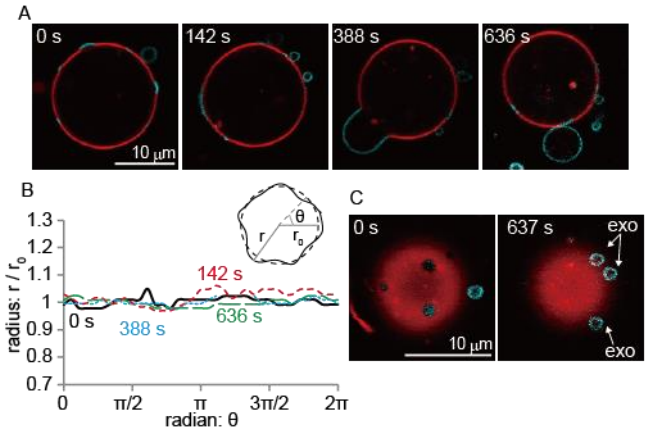

Figure S2. (A) Sectional images of the transformation of heterogeneous membranes after the addition of glucose (2 mM). Time elapsed after treatment. (Red: Ld-phase, Cyan: Lo-phase). (B) The remaining Ld part of the membrane maintained an essentially spherical morphology. The radius r of the mother vesicle was plotted for each θ (θ=2π/n, n=1, 2, …, 36). (C) Typical microscopic images of a vesicle surface before (0 s) and after (637 s) the budding of domains.

3. Deformation pattern of phase-separated membrane.

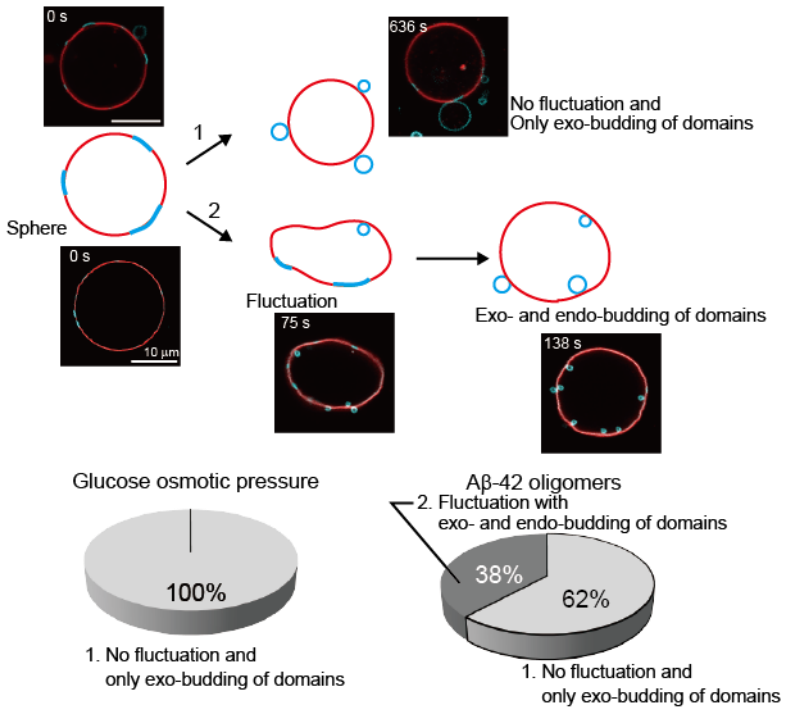

Figure S3. Probability of deformation induced by glucose osmotic pressure (n=12) and Aβ-42 oligomers (n=26).

4. Localization of Aβ-42 monomers and diffusion coefficients of the domain in the presence of Aβ monomers.

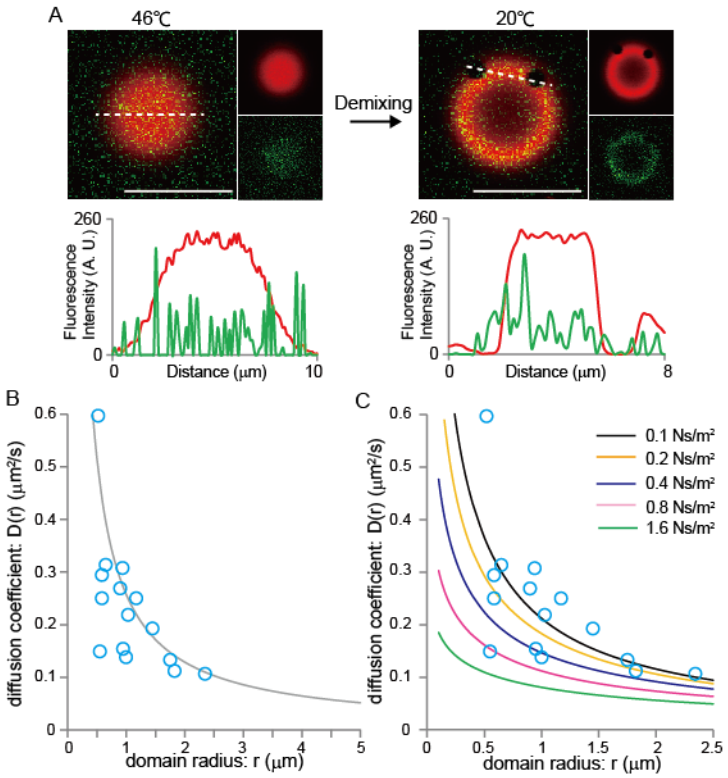

Figure S4. (A) Selective association of Aβ-42 monomers during the mixing/demixing transition. After the membrane phase-separates, Aβ-42 monomers localize in the Ld phase. (B) Diffusion coefficients vs. domain radius with Aβ-42 monomers. The gray solid line fit the Hughes equation. (C) Diffusion coefficients vs. domain radius with Aβ-42 monomers. Solid lines show the theoretical curve given by the Petrov and Schwille equation with increased membrane viscosities.

5. Diffusion coefficients for a domain on a membrane surface

Lo-phase domains diffuse in the Ld-phase via Brownian motion; the diffusion coefficient of a membrane inclusion was originally described by the Saffman and Delbrück equation (1).

$$D(r) = \frac{k_B T}{4\pi\eta''} \left[\ln\left(\frac{\eta''}{\eta_w}\frac{1}{r}\right) - \gamma + 1/2\right] \quad (1)$$

where k_B is the Boltzmann constant, T is the temperature, γ is the Euler constant, and r is the radius of the domain. The hydrodynamics of the system can be characterized by the length scale (λ_0), which is defined as the ratio of the membrane viscosity (η'') to the 3D bulk viscosity of water (η_w), such that $\lambda_0 = \eta''/\eta_w$. 3D membrane viscosity, η''_{3D}, is given by $\eta''_{3D} \approx \eta''/h$, where h is the bilayer thickness. With the use of typical values, $\eta_w \approx 10^{-3}$ [Ns/m^2], $\eta''_{3D} \approx 10^{-1}$ [Ns/m^2] and h $\approx 4 \times 10^{-9}$ [m], we obtain $\eta''/\eta_w \approx 400$ [nm]. For diffusing domains that are on the order of a micrometer in length, diffusion coefficients can be expressed as described by Hughes *et al.* (eq. (2)).

$$D(r) = \frac{k_B T}{16\eta_w}\frac{1}{r} \quad (2)$$

Petrov and Schwille provided an approximation in which they connect eq.(1) and eq.(2):

$$D(\varepsilon) = \frac{k_B T}{4\pi\eta''}\left[\ln(2/\varepsilon) - \gamma + 4\varepsilon/\pi - (\varepsilon^2/2)\ln(2/\varepsilon)\right] \times \left[1 - (\varepsilon^3/\pi)\ln(2/\varepsilon) + C_1\varepsilon^{b1}/(1 + C_2\varepsilon^{b2})\right]^{-1} \quad (3)$$

In the hydrodynamic description, a cylindrical inclusion of radius r is embedded in a membrane with surface viscosity η'', which, in turn, is surrounded by media with bulk viscosities η_{w1} and η_{w2} (outer and inner aqueous phases of the membrane). The corresponding hydrodynamic length scale is $\lambda_0 = \eta''/(\eta_{w1} + \eta_{w2})$, and membrane inclusion is characterized by the reduced radius $\varepsilon = r/\lambda_0 = r(\eta_{w1} + \eta_{w2})/\eta''$. The authors provided the parameters C_1 =0.73761, b_1 =2.74819, C_2 = 0.52119, and b_2 = 0.61465.

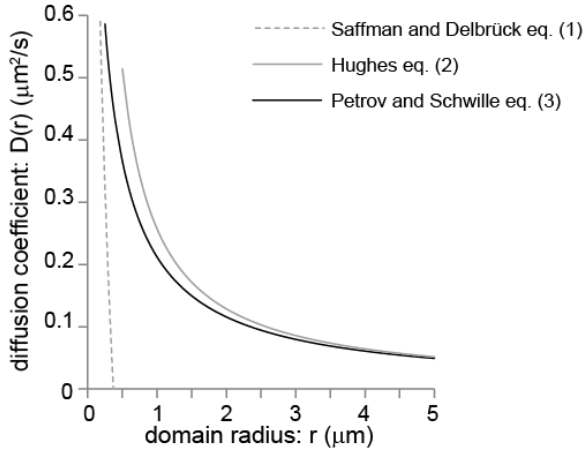

6. Schematic illustration of the time-dependent change in the domain periphery length.

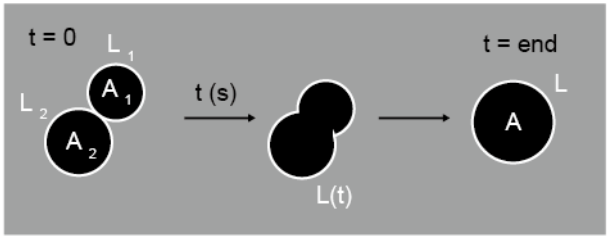

The domain surface area is theoretically constant.

$A = A_1+A_2$

This indicates that the domain periphery length L can be described as

$L = [(L_1)^2+(L_2)^2]^{1/2}$

In addition, $dL = L_1+L_2-L$

Thus, time-dependent change in the domain periphery length can be described as

$[L(t)-L]/dL$.